NOTES AND CORRESPONDENCE

Calculations of Aircraft Contrail Formation Critical Temperatures

MARK L. SCHRADER

Air Weather Service, Scott Air Force Base, Illinois

28 August 1996 and 9 December 1996

ABSTRACT

Forecasts of condensation trail (contrail) formation are an extremely important consideration in military aircraft operations, particularly in the operation of stealth aircraft. Some recently published works have claimed improvements in the time-tested forecast technique of H. Appleman, but the results are called into question by errors in the basic physics. This note provides a brief explanation of contrail formation theory and presents a simple derivation of the critical temperature of contrail formation for representative jet engine types.

1. Introduction

The advent of low-observability ''stealth'' aircraft has made operational forecasting of aircraft condensation trails, or contrails, more important than ever to military aircraft operations. No amount of stealth technology can hide an aircraft if it leaves a persistent contrail in its wake.

Investigations of contrail formation are recorded as early as 1919, and research began in earnest during World War II (Schumann 1996). The definitive work on contrail forecasting is by Appleman (1953). Even today, the original Appleman technique forms the basis of the Air Force Global Weather Center's contrail forecasting algorithm. Recently, some works (Peters 1993; Hanson and Hanson 1995) have claimed improvements in contrail forecasting techniques, but the results are called into question by errors in the basic physics.

This note provides a brief explanation of contrail formation theory and presents a simple derivation of the critical temperature of contrail formation for various jet engine types.

2. Contrail formation

Contrails are clouds that form when a mixture of warm, unsaturated, engine exhaust gases and cold ambient air reaches saturation with respect to water, forming liquid drops, which quickly freeze (Appleman 1953). As ambient air mixes with exhaust gas, the decrease in a wake parcel's absolute humidity is directly proportional to the decrease in its temperature (Iribarne and Godson 1981). This means that the wake parcel approaches ambient conditions along a line with a slope equal to the ratio of the water vapor added by engine exhaust to the increase in temperature caused by the heat added to the parcel by the jet engine, as shown in Fig. 1. The slope of this line is defined as the engine contrail factor and is usually expressed in terms of a water vapor mixing ratio per degree. Published contrail factor values vary from as low as 0.0295 g kg^{-1} K^{-1}

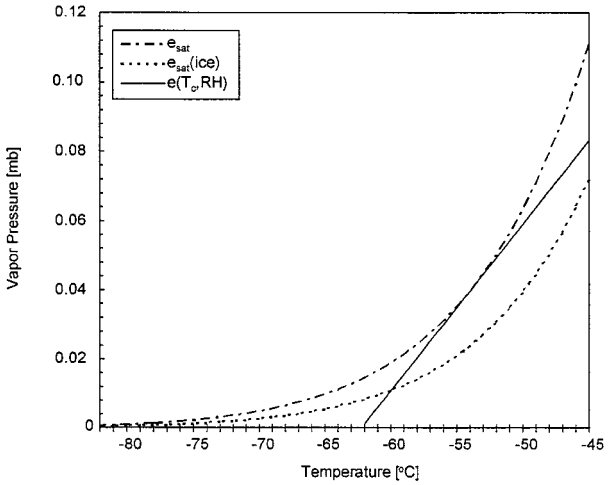

FIG. 1. Saturation vapor pressure with respect to a water surface, e_{sat}, and to an ice surface, e_{sat}(ice). The straight line represents the path along which an aircraft wake parcel returns to ambient conditions for the warmest initial temperatures favorable for contrail formation. In this example, the contrail factor is 0.03 g kg^{-1} K^{-1} and the ambient pressure is 100 mb. The segment of the line from the point tangent to e_{sat} to zero vapor pressure is the set of critical temperatures T_c for all ambient relative humidities.

Corresponding author address: Capt. Mark L. Schrader, 20th Air Support Operations Squadron, 2065 Hangar Access Drive, Fort Drum, NY 13602-5042.
E-mail: 20asos-wx@drum-emh4.army.mil

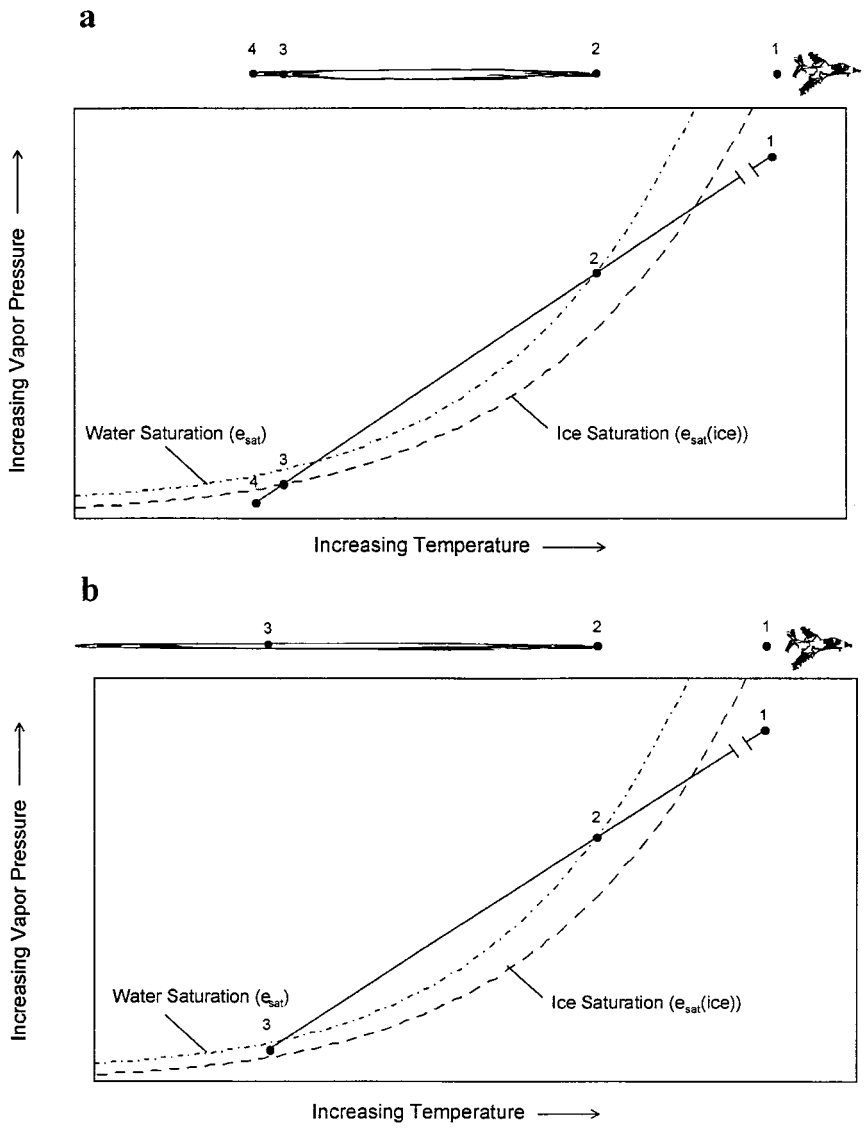

FIG. 2. (a) Example of nonpersistent contrail formation behind a jet aircraft. The numbered points represent a wake parcel at the same point in space at different times. Point 1 represents the exhaust nozzle exit temperature and humidity. The parcel becomes saturated with respect to water at point 2, and the contrail forms. Since the ambient air is unsaturated with respect to ice, the contrail particles sublimate as the parcel returns to ambient conditions between points 3 and 4. (b) As in (a) but for the case of a persistent contrail. The ambient air is saturated with respect to ice, so the contrail is maintained after the wake parcel returns to ambient conditions at point 3.

(Pilié and Jiusto 1958) to as high as 0.049 g kg^{-1} K^{-1} (Peters 1993). The contrail factor formulation of Busen and Schumann (1995) results in a theoretical minimum value of about 0.028 g kg^{-1} K^{-1}. Furthermore, Busen and Schumann (1995) state that the engine contrail factor is not constant but is dependent upon aircraft engine and flight parameters. When making forecasts of contrail formation, however, one must use a representative value for the contrail factor of the engine type under consideration. The maximum temperature at which contrails will form for a given atmospheric relative humidity and at a given pressure level is called the critical temperature T_c. Figures 2a and 2b illustrate contrail formation in an operational context.

3. Critical temperature derivation

The derivation of the critical temperature of contrail formation is straightforward, but some recent works point out the need for greater attention to the basic

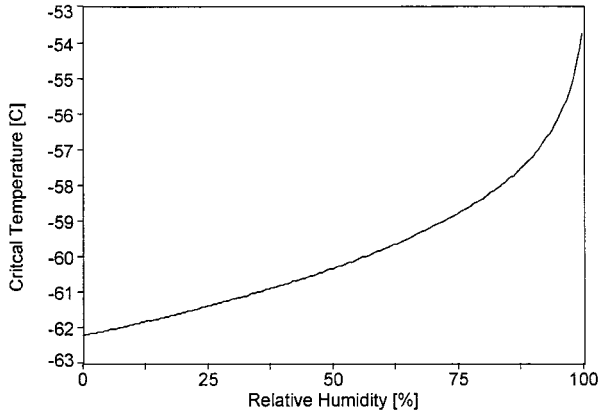

FIG. 3. The variation of critical temperature with relative humidity at 100 mb for a contrail factor of 0.03 g kg^{-1} K^{-1}.

thermodynamics of contrail formation. The technique of Peters (1993) is essentially correct, but the report contains two important errors in this author's opinion. The first is that saturation with respect to ice instead of water is required to form contrails.[1] The second is that a linear interpolation is used to map critical temperatures from vapor pressure–temperature space to relative humidity–temperature space. This results in a linear variation of critical temperature with relative humidity instead of the characteristic variation shown in Fig. 3. In addition, the engine contrail factors cited are significantly higher than more recent results from Northrop–Grumman flight tests (Saatzer 1995). See Schrader et al. (1997) for insights into the approach of Hanson and Hanson (1995).

To derive the critical temperatures for contrail formation, one must first determine the tangent point of the saturation vapor pressure curve (with respect to water) and a line with a slope equal to the contrail factor, converted to units of vapor pressure per degree (see Fig. 1). At this point, the first derivative of the saturation curve is equal to the slope of the path along which an aircraft wake parcel returns to ambient conditions for the warmest possible condition of contrail formation:

$$\frac{d}{dT}e_{\text{sat}}(T) = \text{CF}\frac{p}{622}, \tag{1}$$

where $e_{\text{sat}}(T)$ (mb) is the saturation vapor pressure with respect to water, CF(g kg^{-1} K^{-1}) is the contrail factor, and p (mb) is the atmospheric pressure. The temperature that satisfies Eq. (1) is the critical temperature at an ambient relative humidity of 100%, $T_{c,100}$. The next step is to find the critical temperature at any relative humidity $T_{c,\text{RH}}$.

The equation for the line of critical temperatures can be defined since a point on the line ($T_{c,100}$) and its slope, which is equivalent to the engine contrail factor (in units of vapor pressure per degree), are known. The equation for this line is

$$e(T_{c,\text{RH}}) = e_{\text{sat}}(T_{c,100}) - (T_{c,100} - T_{c,\text{RH}})\left.\frac{de_{\text{sat}}}{dT}\right|_{T_{c,100}}. \tag{2}$$

Using Eq. (2) in an approximate equation for relative humidity (valid for $e_{\text{sat}} \ll p$),

$$\frac{e(T_{c,\text{RH}})}{e_{\text{sat}}(T_{c,\text{RH}})} = \frac{\text{RH}}{100},$$

yields the expression

$$\frac{e_{\text{sat}}(T_{c,100}) - (T_{c,100} - T_{c,\text{RH}})\left.\frac{de_{\text{sat}}}{dT}\right|_{T_{c,100}}}{e_{\text{sat}}(T_{c,\text{RH}})} = \frac{\text{RH}}{100}. \tag{3}$$

This equation can be solved iteratively to find the critical temperature for any relative humidity $T_{c,\text{RH}}$ and any pressure level.

4. Results

Appleman diagrams for specific engine types (Saatzer 1995) are shown in Figs. 4a–c. Tables are provided in the appendix. Contrail factors for bypass engines are higher than those for nonbypass engines because the core exit temperature is reduced by extracting some energy to turn the fan.

The sensitivity of the forecast to temperature uncertainty is illustrated by the narrow critical temperature range (~3°C) between 0% and 70% ambient relative humidity. Within this region, contrail forecast errors are dominated by errors in forecast temperature and are relatively unaffected by humidity uncertainty. At relative humidities higher than about 70%, contrail forecast errors are dominated by uncertainties in the forecast relative humidity. The work of Busen and Schumann (1995) further points out the need to consider uncertainties in the contrail factor in addition to forecast variables.

5. Summary

The formation of contrails behind military aircraft is an important consideration in military operations. Even mildly persistent contrails will compromise an otherwise stealthy aircraft. While some recent works claim improvements to the traditional methods of contrail forecasting, the method of Appleman (1953), tailored to the specific engine type of the aircraft under consideration, remains the best for operational contrail forecasting. A straightforward derivation of contrail formation critical temperature has been presented using the isobaric mixing model put forth by Appleman.

[1] Although Peters (1993) correctly states that water saturation is required to form contrails, Peters's Eq. (2) is actually the Goff–Gratch formulation for saturation over an ice surface given by List (1966).

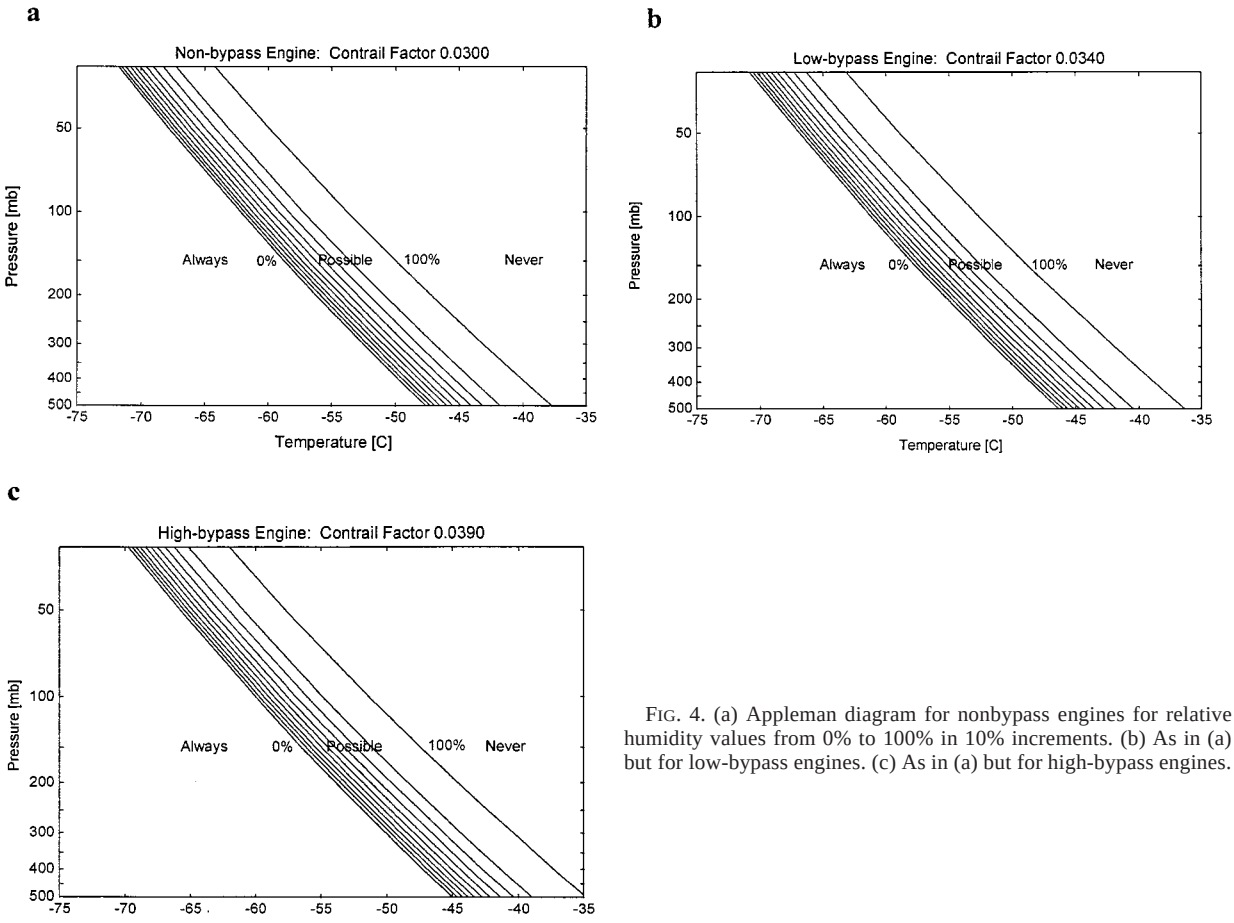

FIG. 4. (a) Appleman diagram for nonbypass engines for relative humidity values from 0% to 100% in 10% increments. (b) As in (a) but for low-bypass engines. (c) As in (a) but for high-bypass engines.

REFERENCES

Appleman, H., 1953: The formation of exhaust condensation trails by jet aircraft. *Bull. Amer. Meteor. Soc.,* **34,** 14–20.

Busen, R., and U. Schumann, 1995: Visible contrail formation from fuels with different sulfur contents. *Geophys. Res. Lett.,* **22,** 1357–1360.

Hanson, H. M., and D. M Hanson, 1995: A reexamination of the formation of exhaust condensation trails by jet aircraft. *J. Appl. Meteor.,* **34,** 2400–2405.

Iribarne, J. V., and W. L. Godson, 1981: *Atmospheric Thermodynamics.* 2d ed. D. Reidel Publishing, 128 pp.

List, R. J., 1966: *Smithsonian Meteorological Tables.* 6th ed. Smithsonian Institution, 527 pp.

Peters, J. L., 1993: New techniques for contrail forecasting. AWS/TR-93/001, 26 pp. [Available from HQ Air Weather Service, Scott Air Force Base, IL 62225.]

Pilié, R. J., and J. E. Jiusto, 1958: A laboratory study of contrails. *J. Meteor.,* **15,** 149–154.

Saatzer, P., 1995: Pilot alert system flight test. Final Rep., 241 pp. [Available from Northrop Grumman, 8900 East Washington Blvd, Pico Rivera, CA 90660-3783.]

Schrader, M. L., W. D. Meyer, and C. L. Weaver, 1997: Comments on ''A reexamination of the formation of exhaust condensation trails by jet aircraft.'' *J. Appl. Meteor.,* **36,** 623–626.

Schumann, U., 1996: On conditions for contrail formation from aircraft exhausts. *Meteor. Z.,* **N. F. 5,** 3–22.

APPENDIX

Critical Temperature Tables

TABLE A1. Critical temperatures for a contrail factor of 0.0336 g kg^{-1} (according to Appleman).

Pressure (mb)	Humidity 0%	10%	20%	30%	40%	50%	60%	70%	80%	90%	100%
30	−70.92	−70.65	−70.35	−70.01	−69.65	−69.23	−68.75	−68.17	−67.44	−66.41	−63.30
50	−66.97	−66.68	−66.36	−66.02	−65.63	−65.19	−64.69	−64.08	−63.32	−62.23	−58.97
100	−61.29	−60.98	−60.64	−60.27	−59.86	−59.39	−58.85	−58.21	−57.39	−56.23	−52.74
150	−57.78	−57.46	−57.11	−56.73	−56.30	−55.81	−55.25	−54.58	−53.73	−52.52	−48.89
200	−55.21	−54.88	−54.52	−54.12	−53.68	−53.18	−52.61	−51.91	−51.04	−49.80	−46.07
250	−53.16	−52.82	−52.46	−52.05	−51.60	−51.09	−50.50	−49.79	−48.90	−47.63	−43.81
300	−51.46	−51.11	−50.74	−50.32	−49.86	−49.34	−48.74	−48.02	−47.11	−45.82	−41.93
400	−48.70	−48.34	−47.96	−47.53	−47.06	−46.52	−45.90	−45.16	−44.22	−42.89	−38.88
500	−46.50	−46.14	−45.74	−45.31	−44.82	−44.27	−43.64	−42.88	−41.92	−40.56	−36.46

TABLE A2. Critical temperatures for a contrail factor of 0.0300 g kg^{-1} K^{-1} (nonbypass).

Pressure (mb)	Humidity 0%	10%	20%	30%	40%	50%	60%	70%	80%	90%	100%
30	−71.78	−71.50	−71.20	−70.88	−70.51	−70.10	−69.62	−69.05	−68.33	−67.31	−64.23
50	−67.86	−67.58	−67.26	−66.92	−66.54	−66.11	−65.61	−65.01	−64.25	−63.18	−59.95
100	−62.24	−61.94	−61.60	−61.24	−60.83	−60.37	−59.83	−59.20	−58.39	−57.24	−53.79
150	−58.78	−58.46	−58.11	−57.73	−57.31	−56.83	−56.27	−55.61	−54.77	−53.57	−49.99
200	−56.23	−55.91	−55.55	−55.16	−54.72	−54.23	−53.66	−52.97	−52.11	−50.88	−47.19
250	−54.21	−53.87	−53.51	−53.11	−52.66	−52.16	−51.58	−50.88	−49.99	−48.73	−44.96
300	−52.52	−52.18	−51.81	−51.40	−50.95	−50.43	−49.84	−49.13	−48.23	−46.95	−43.10
400	−49.79	−49.44	−49.06	−48.64	−48.17	−47.64	−47.03	−46.30	−45.37	−44.05	−40.10
500	−47.62	−47.26	−46.87	−46.44	−45.96	−45.42	−44.80	−44.05	−43.10	−41.75	−37.70

TABLE A3. Critical temperatures for a contrail factor of 0.0340 g kg^{-1} K^{-1} (low bypass).

Pressure (mb)	Humidity 0%	10%	20%	30%	40%	50%	60%	70%	80%	90%	100%
30	−70.83	−70.56	−70.26	−69.92	−69.56	−69.14	−68.66	−68.08	−67.35	−66.31	−63.20
50	−66.88	−66.59	−66.27	−65.92	−65.54	−65.10	−64.59	−63.99	−63.22	−62.13	−58.87
100	−61.19	−60.88	−60.54	−60.17	−59.76	−59.29	−58.75	−58.10	−57.28	−56.12	−52.63
150	−57.68	−57.36	−57.01	−56.62	−56.19	−55.71	−55.14	−54.47	−53.62	−52.41	−48.78
200	−55.10	−54.77	−54.41	−54.01	−53.57	−53.07	−52.49	−51.80	−50.93	−49.68	−45.95
250	−53.05	−52.71	−52.35	−51.94	−51.49	−50.98	−50.39	−49.68	−48.78	−47.51	−43.69
300	−51.34	−51.00	−50.62	−50.21	−49.75	−49.23	−48.63	−47.91	−47.00	−45.70	−41.81
400	−48.58	−48.23	−47.84	−47.41	−46.94	−46.40	−45.79	−45.04	−44.10	−42.77	−38.76
500	−46.38	−46.02	−45.62	−45.19	−44.70	−44.15	−43.52	−42.76	−41.80	−40.43	−36.33

TABLE A4. Critical temperatures for a contrail factor of 0.0390 g kg^{-1} K^{-1} (high bypass).

Pressure (mb)	Humidity 0%	10%	20%	30%	40%	50%	60%	70%	80%	90%	100%
30	−69.79	−69.51	−69.20	−68.87	−68.50	−68.07	−67.58	−67.00	−66.26	−65.21	−62.06
50	−65.78	−65.49	−65.17	−64.81	−64.42	−63.98	−63.47	−62.85	−62.08	−60.98	−57.67
100	−60.02	−59.70	−59.36	−58.98	−58.57	−58.09	−57.55	−56.89	−56.06	−54.88	−51.35
150	−56.46	−56.13	−55.78	−55.39	−54.95	−54.46	−53.89	−53.21	−52.35	−51.12	−47.44
200	−53.85	−53.51	−53.15	−52.74	−52.30	−51.79	−51.20	−50.50	−49.62	−48.35	−44.57
250	−51.77	−51.43	−51.05	−50.64	−50.18	−49.67	−49.07	−48.35	−47.44	−46.15	−42.28
300	−50.04	−49.69	−49.31	−48.89	−48.42	−47.89	−47.28	−46.55	−45.63	−44.31	−40.36
400	−47.23	−46.87	−46.48	−46.05	−45.57	−45.03	−44.40	−43.65	−42.69	−41.34	−37.27
500	−45.00	−44.63	−44.23	−43.79	−43.30	−42.74	−42.10	−41.33	−40.35	−38.97	−34.80